

STEREO RADARGRAMMETRY WITH DIGITAL SIDE-LOOKING RADAR IMAGES

J. WU, D. C., LIN AND D. K. CHEN

CENTER FOR SPACE AND REMOTE SENSING RESEARCH
NATIONAL CENTRAL UNIVERSITY
CHUNG-LI, TAIWAN, ROC, 32054

XVII ISPRS CONGRESS IN WASHINGTON, D.C.
COMM. II , AUGUST 2-14, 1992

ABSTRACT

With self-calibrating parameters in polynomials, basic radargrammetric conditions are extended to allow for residual systematic errors in side-looking radar (SLR) imagery. In a further attempt, we apply a statistical interpolation method, that of linear prediction with filtering, to describing time-varying orientation parameters. We document briefly this algorithmic development over the last 4 years at our Center. It is felt we implicitly take advantage of some experiences gathered in geometric analysis on optical remote sensing imagery.

Using stereoscopic real-aperture side-looking airborne radar images over a hilly area near Taipei, we conduct tests about the effects resulting from functional models extended for SLR point determination. While rather limited accuracy data are obtained, we learn that weight constraints on over hundreds of unknown parameters are very important to radargrammetric processing for positions.

Key Words : Extended radargrammetric equations, Modeling for time-dependent parameters.

1. INTRODUCTION

Radargrammetric conditions for side-looking radar (SLR) imagery have been known for quite some time, see Derenyi(1974), Leberl(1979), Norvelle(1972) and Raggam(1988). In our basic radargrammetric equations, we apply piecewise continuous linear models to time-dependent position and attitude parameters at SLR(real-aperture) antenna stations. In an attempt to extend radargrammetric conditions, the cross-track image scale is no longer considered as being constant; besides, we add self-calibrating parameters in polynomials to the basic equations. This functional extension leads to more or less improvement in accuracy at independent check points when a

pair of stereo SLR images are processed for object-space 3D multi-point positions. In a further algorithmic attempt, use is made of a statistical interpolation method, also called the method of linear prediction, to describe the time-dependent orientation parameters along flight routes. We give concise descriptions about the applied theories at different stages and report a set of comparable results achieved.

2. EXTENDED RADARGRAMMETRIC EQUATIONS

Geometrically, image-forming of side-looking radar is characterized in azimuth and in range directions by

$$x_i = m_{x_i} [\cos \phi_j \cos \kappa_j (X_i - X_{o_j}) + \sin \kappa_j (Y_i - Y_{o_j}) - \sin \phi_j \cos \kappa_j (Z_i - Z_{o_j})] = m_{x_i} \mathbf{a}^T \mathbf{r} \quad (1a)$$

$$y_i = m_{y_i} [(|\mathbf{r}|^2 - H^2)^{1/2} - D] \quad (1b)$$

where

- x_i, y_i : instantaneous along-track and cross-track image coordinates of point i ; $x_i = 0$ meaning a systematic squint assumed to be zero;
- m_{x_i}, m_{y_i} : image scale factors in azimuth and range directions, respectively;
- X_i, Y_i, Z_i : object-space coordinates of point i ;
- $X_{o_j}, Y_{o_j}, Z_{o_j}$: time-dependent positions of SLR (real-aperture) antenna at station j when point target i is scanned;
- ϕ_j, κ_j : time-dependent pitch and yaw parameters at station j ;
- H : average flying altitude above ground;
- D : delay for ground range measurements.

Where c_y and d_y are again seen as relative intervals. Instead of one scale parameter, we get several cross-track scale parameters $\dots m_{y_n}, m_{y_{n+1}} \dots$ subject to iterative least squares estimation. In addition, we apply self-calibrating parameters $a_0 \dots b_4$ to reduce residual systematic errors in SLR images as follows (Wu and Chen, 1990):

In order to avoid abrupt changing in slopes associated with piecewise linear modeling functions in Eq.(1c), we adopt a statistical method, that of least squares interpolation (Kraus and Mikhail, 1972), as models for differential time-dependent parameters:

$$x_i + a_0 + a_1 s_i + a_2 s_i y_i = m_{x_i} \mathbf{a}^T \mathbf{r}, \text{ letting } x_i = 0 \quad (2b)$$

$$y_i + b_0 + b_1 s_i + b_2 s_i y_i + b_3 s_i^2 y_i + b_4 s_i y_i^2 = m_{y_i} [(|\mathbf{r}|^2 - H^2)^{1/2} - D] \quad (2c)$$

Piecewise continuous linear models for the time-dependent parameters used are:

$$\begin{aligned} X_{o_j} &= (1 - c/d)X_{o_k} + (c/d)X_{o_{k+1}} \\ Y_{o_j} &= (1 - c/d)Y_{o_k} + (c/d)Y_{o_{k+1}} \\ Z_{o_j} &= (1 - c/d)Z_{o_k} + (c/d)Z_{o_{k+1}} \quad (1c) \\ \phi_j &= (1 - c/d)\phi_k + (c/d)\phi_{k+1} \\ \kappa_j &= (1 - c/d)\kappa_k + (c/d)\kappa_{k+1} \end{aligned}$$

Here, c is a relative interval in units of time or length between SLR stations j and k ; d is the separation in the same units between stations k and $k + 1$. Eq.(1) stands for our basic radargrammetric conditions in which image scales m_{x_i}, m_{y_i} are both constants; and one attitude parameter, roll, is explicitly excluded for fear of its geometric correlation with Y_{o_j} .

In a functional extension of Eq.(1), we allow m_{y_i} to vary piecewise linearly:

$$m_{y_i} = (1 - c_y/d_y)m_{y_n} + (c_y/d_y)m_{y_{n+1}} \quad (2a)$$

$$\begin{aligned} dX_{o_j} &= \mathbf{c}_{jk}^T \mathbf{C}_{kk}^{-1} d\mathbf{X}_{o_k} \\ dY_{o_j} &= \mathbf{c}_{jk}^T \mathbf{C}_{kk}^{-1} d\mathbf{Y}_{o_k} \\ dZ_{o_j} &= \mathbf{c}_{jk}^T \mathbf{C}_{kk}^{-1} d\mathbf{Z}_{o_k} \\ d\phi_j &= \mathbf{c}_{jk}^T \mathbf{C}_{kk}^{-1} d\phi_k \\ d\kappa_j &= \mathbf{c}_{jk}^T \mathbf{C}_{kk}^{-1} d\kappa_k \end{aligned} \quad (3)$$

Here, \mathbf{c}_{jk} is a covariance vector; \mathbf{C}_{kk} a covariance matrix. Knowing relative intervals in time or length between SLR stations $\dots k - 1, k, j, k + 1, \dots$, we can calculate the covariance vector and matrix from empirical covariance functions, such as $c(d) = c_0 \cdot \exp(-h^2 d^2)$.

We have now at our hand three functional models of different algorithmic complexity. Eqs.(1a, 1b, 1c) represent the basic one which is designated as Model-I. Putting Eqs.(2a, 2b, 2c and 1c) together, we get an extended radargrammetric equations, Model-II. When we combine Eqs.(2a, 2b, 2c) with Eq.(3), a further extended function, Model-III, is formed. It is noteworthy that the Models-I, II, III are all applicable to side-looking radar imagery, either monoscopically for space resection or stereoscopically for concurrent space resection and intersection.

3. TESTS WITH SIDE-LOOKING AIRBORNE RADAR IMAGES

An area of $24 \times 15 \text{ km}^2$ with height differences reaching 611 m is selected for testing the before-mentioned Models. Stereoscopic same-side images of the area in ground range projection (Fig.1) were acquired by a side-looking airborne radar at 510 km/hr in 1981 with

length of real-aperture antenna : 588 cm;
 wavelength in X-band : 3 cm;
 duration of radar pulses : $0.2 \mu\text{sec}$;
 range resolution at 70° off-nadir : 32 m;
 azimuth resolution at 70° off-nadir : 57 m ;
 range delay D prior to image recording : 10 km;
 average flying altitude H above ground : 5 km ;
 nominal image scales : $1/250\ 000$.

Conjugate points on digitized images and on $1:25\ 000$ are identified and measured manually. The following a priori standard deviations are

used for observations and parameters so that they can be weighted accordingly:

measurement precision for image coordinates (variance of unit weight) : $\pm 30 \mu\text{m}$;

ground control coordinates : $\pm 50 \text{ m}$;

at SLR antenna station k's

pitch ϕ_k : $\pm 0.05 \text{ rad}$;

yaw κ_k : $\pm 0.10 \text{ rad}$;

positions X_{o_k}, Y_{o_k} : $\pm 500 \text{ m}$;

height above datum Z_{o_k} : $\pm 250 \text{ m}$;

cross-track image scales : $\pm 4.1 \times 10^{-7}$.

There are 3 SLR antenna stations chosen for each of the two flight lines, producing a total of $2 \times (3 \times 5) = 30$ unknown position and attitude parameters. For every SLAR image strip, use of three cross-track image scale factors is made in Models-II or III, in total 6 scale parameters.

In general, it takes about 11 iterations to fulfil numerically nonlinear Eqs. (1a,1b) or (2b,2c) to

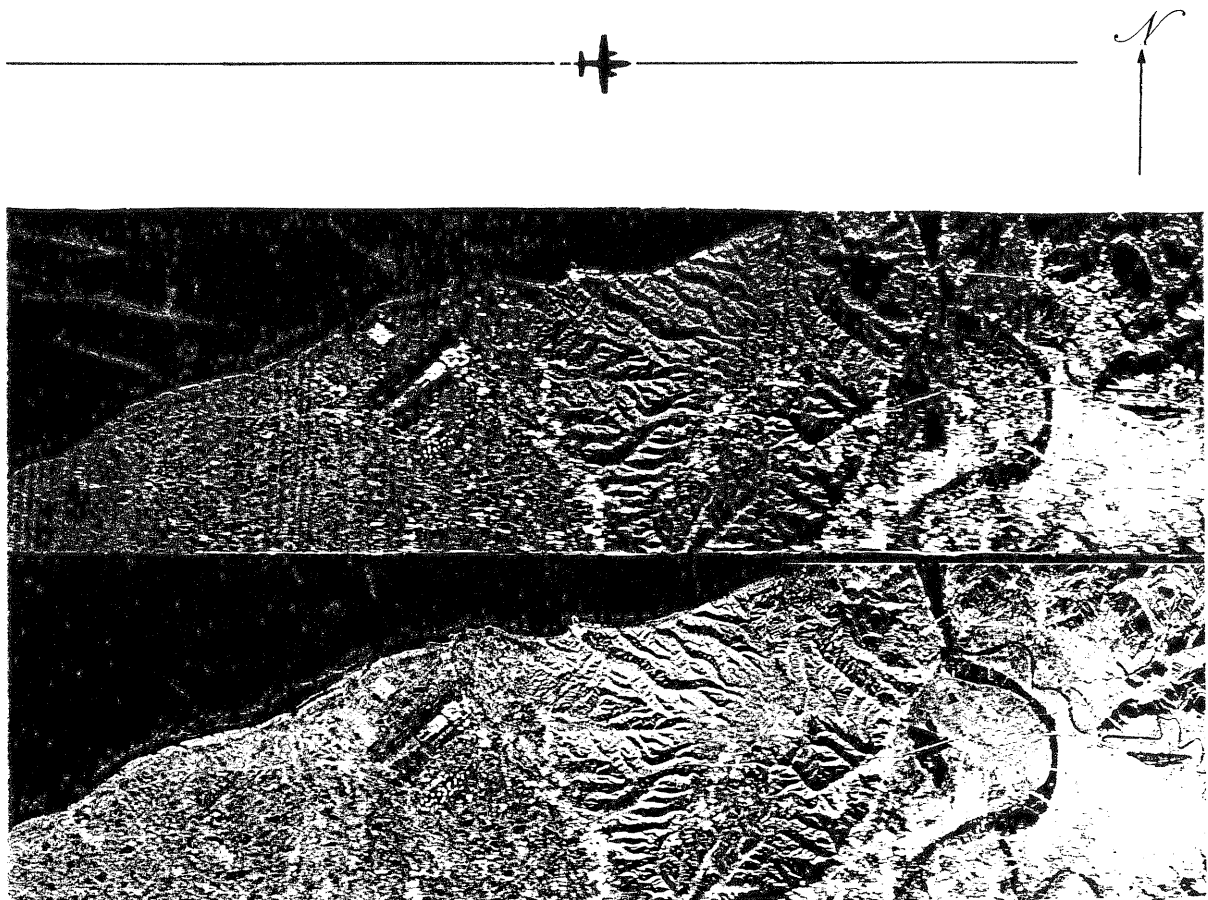


Fig.1. Stereoscopic side-looking radar images with $2.5^\circ - 10^\circ$ stereo intersection angles; to the west of Taipei.

Table 1. Accuracies in X, Y, Z at 50 independent check points using 25 evenly distributed ground control points.

Model-I			Model-II			Model-III					
						$c_0 = 0.9999$			$c_0 = 0.765^*$		
						$h = 0.0012$			$h = 0.012^*$		
X	Y	Z	X	Y	Z	X	Y	Z	X	Y	Z
74.7	69.7	111.2	73.5	66.9	106.0	73.5	68.6	104.0	73.3	62.9	88.7

* Using the method of linear prediction with filtering

within 6.5×10^{-5} . We give here as an example in Table 1 a comparison in performance between the Models-I, -II and -III.

Out of recent analysis and up to now, we may conclude that for SLR same-side stereo images Model-II is (slightly) better than Model-I, and Model-III is better, if not compatible, than Model-II. Since the total number of unknown parameters reaches 277 in study cases for Table 1, weighting for "observed" parameters in least squares estimation deserves great attention.

4. DISCUSSIONS AND OUTLOOKS

Our functional models for analyzing real-aperture side-looking radar imagery are explained and a preliminary finding on differences between the models presented. Extending functional models is in essence algorithmic. However, we believe that improvements on accuracies in height are limited by stereo intersection angles reaching from 2.5° to 10° in our overlapping images and limited by their ground resolutions having 112 m in azimuth at far ranges. In the near future, we intend to include another SLR image strip in opposite-side geometry which shows less acute stereo intersection angles. It can mean that more accurate 3D positioning is achievable. Even though it remains doubtful to generate high-quality digital elevation models with microwave imagery from side-looking radar, we have demonstrated how time-dependent orientation parameters can be effectively estimated by resorting to geometric control information on the ground. The parameters then find applications

to digital rectification of SLR images, given a dense digital elevation model (derived e.g. from aerial photogrammetry). SLR orthographic images thus obtained are invaluable to vertical overlay analysis in thematic mapping. Lastly, research funds granted by the Council of Agriculture are gratefully acknowledged.

5. REFERENCES

- Derenyi, E.E., 1974. SLAR geometric test. Photogrammetric Engineering 40, pp.597-604.
- Kraus, K. and Mikhail, E.M., 1972. Linear least-squares Interpolation. XII. ISP Congress in Ottawa, Comm. III, 14 pages.
- Leberl, F., 1979. Accuracy analysis of stereo side-looking radar. Photogrammetric Engineering and Remote Sensing 45(8), pp.1083-1096.
- Norvelle, F.R., 1972. AS-11A radar program. Photogrammetric Engineering 38(1), pp.77-82.
- Raggam, J., 1988. An efficient object space algorithm for spaceborne SAR image geocoding. Int. Arch. Photogramm. Remote Sensing 27(B11), pp.II-393—II-400.
- Wang, Z.Z., 1990. Principles of Photogrammetry (with Remote Sensing). Publishing House of Surveying and Mapping, Beijing, pp.462-484.
- Wu, J. and Chen, D.K., 1990. Topographic photo-maps from stereoscopic side-looking radar images in digital format. Int. Arch. Photogramm. Remote Sensing 28(4), pp.570-579.